

Enhanced atom transfer in a double magneto-optical trap setup

S. R. Mishra,* S. P. Ram, S. K. Tiwari, and S. C. Mehendale

Laser Physics Applications Division, Raja Ramanna Centre for Advanced Technology, Indore 452013, India

(Received 19 February 2008; published 19 June 2008; publisher error corrected 25 June 2008)

We report the observation of significant enhancement in the transfer of laser-cooled ^{87}Rb atoms between two vertically separated magneto-optical traps (MOTs) when an appropriately tuned and aligned hollow laser beam was used. In the experimental setup, the lower MOT was loaded from a continuous flux of atoms ejected from the upper MOT by a resonant push beam. The observed enhancement appears to be mainly due to a slowing down of atoms by the hollow beam after being ejected from the upper MOT.

DOI: [10.1103/PhysRevA.77.065402](https://doi.org/10.1103/PhysRevA.77.065402)

PACS number(s): 37.10.De, 37.10.Gh, 37.10.Vz

The magneto-optical trap (MOT) has emerged as a very convenient source of cold atoms for experimental research in several areas such as Bose-Einstein condensation (BEC), atom optics, quantum optics, cold-atom collisions, degenerate Fermi-gases, and quantum metrology [1–17]. To achieve BEC of alkali metal and alkaline-earth metal atoms, these are initially cooled in a MOT and then undergo evaporative cooling in a magnetic trap to reach a temperature lower than the critical temperature for BEC [3]. The vapor cell MOT, in which atoms to be cooled and trapped are derived from background atoms, is a very convenient design for the first step. However, as evaporative cooling is a slow process, the second step requires a much better vacuum than that in this type of MOT to achieve the required trap lifetime. One way to overcome these conflicting requirements is to use the double-MOT design [18,19] in which atoms trapped in the vapor cell MOT are transferred to another MOT in an ultrahigh-vacuum (UHV) chamber. Various methods such as moving magnetic coils [20,21], imbalance of trapping beams forces [22], or use of a push beam [18,23,24] are employed to transfer atoms from one MOT to another. Efficient transfer of atoms from one MOT to another is clearly of prime importance in double-MOT systems. To enhance the transfer efficiency, use of two-dimensional cooling [23], guiding magnetic fields [18], and guiding laser beams [25] during the transfer has been reported. Here we report that a hollow laser beam can be used to enhance atom transfer between two MOTs. A weakly focused hollow laser beam propagating opposite to the direction of the ejected atomic flux was aligned such that both MOTs were in the dark region of the hollow beam. Significant enhancement in the number of atoms in the lower UHV MOT was observed in the presence of the hollow beam when it was tuned near the cooling transition. Since hollow beams can be easily generated with high efficiency [26], our approach may prove to be an easy option to enhance the number of atoms in a MOT for experiments where the initial number matters, such as evaporative cooling to achieve BEC.

Figure 1 shows a schematic of the experimental setup used. The upper MOT was formed in an octagonal stainless-steel chamber, while the lower MOT was formed inside a quartz glass cell (polished but uncoated) connected to the

bottom of another chamber. This chamber was connected to the upper chamber by a tapered tube [differential pumping tube (DPT): inner diameters of 5.0 mm and 12.0 mm at the ends] which allowed differential pumping and provided convenient passage for the converging hollow beam propagating in an upward direction. The upper MOT and the lower MOT positions were vertically separated by ~ 340 mm. With suitable vacuum pumps, base pressures of $\sim 1 \times 10^{-8}$ Torr and $\sim 1.2 \times 10^{-9}$ Torr were obtained in the upper and lower chambers, respectively. On heating a Rb getter in the upper chamber, Rb vapor was generated and the pressure in the chamber increased to $\sim 2 \times 10^{-8}$ Torr. The vapor pressure in the chamber was limited by the getter current and pumping rate, and was not optimized.

The cooling laser beams for the two MOTs were obtained from two separate grating-controlled external-cavity diode lasers and the repumping laser beams were obtained by di-

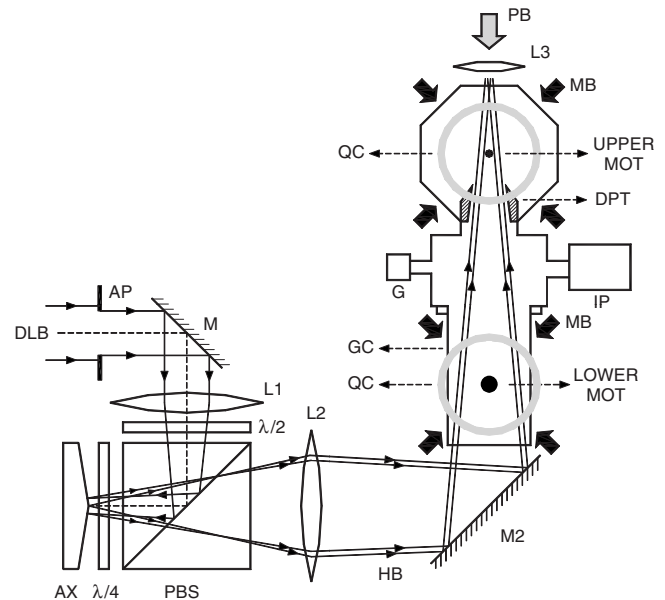


FIG. 1. Schematic of the experimental setup. DLB: diode laser beam. AX: axicon mirror. $\lambda/2$: half-wave plate. $\lambda/4$: quarter-wave plate. PBS: polarizing beam splitter. L1, L2, and L3: lenses of 80 mm, 250 mm, and 300 mm focal length. HB: hollow beam. MB: MOT beams. PB: push beam. IP: sputter ion pump. G: vacuum gauge. GC: glass cell. QC: quadrupole coil. DPT: differential pumping tube.

*srm@cat.ernet.in

viding the output from a single laser of a similar configuration. For each MOT, the cooling beam and the repumping beam were first mixed, and the combined beam was then expanded and split into three MOT beams, which entered the chamber. After retroreflection of each of these three beams by a mirror at the exit of the chamber, the required six MOT beams were obtained. For the upper MOT, the total power in the three beams (each of diameter 10 mm) entering the chamber was ~ 26 mW (with ~ 17 mW in the cooling part and ~ 9 mW in the repumping part). For the lower MOT, the total power in the three beams (each of diameter 7 mm) was ~ 27 mW (with ~ 18 mW in the cooling part and ~ 9 mW in the repumping part). All lasers were locked using hyperfine absorption signals generated by saturated absorption spectroscopy (SAS). The cooling laser was locked at the side of the hyperfine absorption peak at the desired detuning using a suitable reference voltage. The repumper laser was stabilized at the peak using a frequency modulation (FM) scheme to generate a dispersive-like signal. The cooling lasers were locked at ~ 12 MHz to the red of $5S_{1/2}F=2 \rightarrow 5P_{3/2}F'=3$ transition of ^{87}Rb , whereas repumper laser was locked at peak of its $5S_{1/2}F=1 \rightarrow 5P_{3/2}F'=2$ transition. The required polarizations of the MOT beams were set using quarter-wave plates. Quadrupole coils (QCs) generated axial magnetic field gradients of ~ 12 G/cm in the upper MOT and ~ 10 G/cm in the lower MOT.

The push beam was a continuous-wave Gaussian laser beam resonant with a $5S_{1/2}F=2 \rightarrow 5P_{3/2}F'=3$ transition of ^{87}Rb . It was focused to a $1/e^2$ size of ~ 100 μm at the upper MOT position, which corresponded to a push beam intensity at the upper MOT of $\sim 10^3$ mW/cm 2 and at the lower MOT of ~ 13 mW/cm 2 for a power of ~ 150 μW . Atoms ejected from the upper MOT by the push beam were captured in the lower MOT. A weakly focused hollow laser beam propagating vertically upwards was aligned such that both MOTs were in its dark central region. The hollow beam was generated using a homemade metal axicon mirror (AX), as reported earlier [26]. As shown in Fig. 2, the peak-to-peak intensity diameter and ring width [full width at half maximum (FWHM)] of the hollow beam were, respectively, ~ 14.3 mm and ~ 1.4 mm at the lower MOT and ~ 3.2 mm and ~ 1.24 mm at the upper MOT. This corresponds to peak intensities at the lower and upper MOT planes of ~ 50 mW/cm 2 and ~ 230 mW/cm 2 , respectively, for a beam power of 30 mW.

We estimated the number of atoms in the two MOTs by analyzing fluorescence images obtained with a digital charge-coupled device (CCD) camera as reported earlier [27]. The number of atoms (N) was obtained using the relation [28]

$$N = \frac{8\pi \left[1 + 4 \left(\frac{\Delta}{\Gamma} \right)^2 + \left(6 \frac{I_0}{I_{\text{sat}}} \right) \right]}{\Gamma \left(6 \frac{I_0}{I_{\text{sat}}} \right) t_{\text{exp}} \eta \Omega} N_c, \quad (1)$$

where N_c is the total number of counts in the image, t_{exp} is the CCD exposure time, η is the CCD quantum efficiency, I_{sat} is the saturation intensity, I_0 is the intensity of each cool-

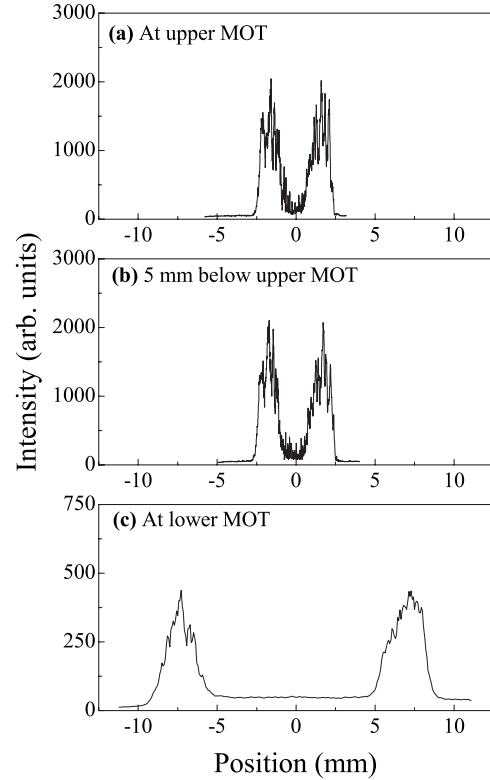


FIG. 2. Intensity profiles of the hollow beam at different positions: (a) at the upper MOT, (b) at 5 mm below the upper MOT, and (c) at the lower MOT.

ing beam in the MOT, $\Gamma = 2\pi \times 6$ MHz is the ^{87}Rb natural linewidth, Δ is the detuning of the cooling beam, and Ω is a solid angle for the collection of fluorescence by the CCD.

In the absence of the push beam and the hollow beam, the upper MOT had $\sim 1.4 \times 10^6$ atoms, whereas the lower MOT did not have a measurable number of atoms. After switching the push beam on, atoms were ejected from the upper MOT and trapped in the lower MOT. The number of atoms in the lower MOT varied with push beam power (ranging from 10 μW to 200 μW), and the maximum number of trapped atoms was achieved for power ~ 160 μW .

Upon switching the hollow beam also on, the number of atoms in the lower MOT changed significantly and the change depended on both the power as well as the frequency of the hollow beam. Figures 3(a) and 3(b) show the observed variation of number of atoms in the lower MOT with hollow beam frequency detuning (δ) from the cooling transition for two powers of the hollow beam and a constant push beam power of 160 μW . The horizontal lines in the figure show the atom number in the lower MOT in the absence of the hollow beam. As can be seen from Fig. 3, a significant enhancement in the number of atoms in the lower MOT was observed for certain ranges of both positive and negative detunings of the hollow beam frequency. The cold-atom cloud was destroyed when the frequency was resonant with $F=2 \rightarrow F'=2,3$ transitions. To know whether the hollow beam had any effect on the upper MOT, we also measured the number of atoms in the upper MOT in the presence of the hollow beam after blocking the push beam. The observed

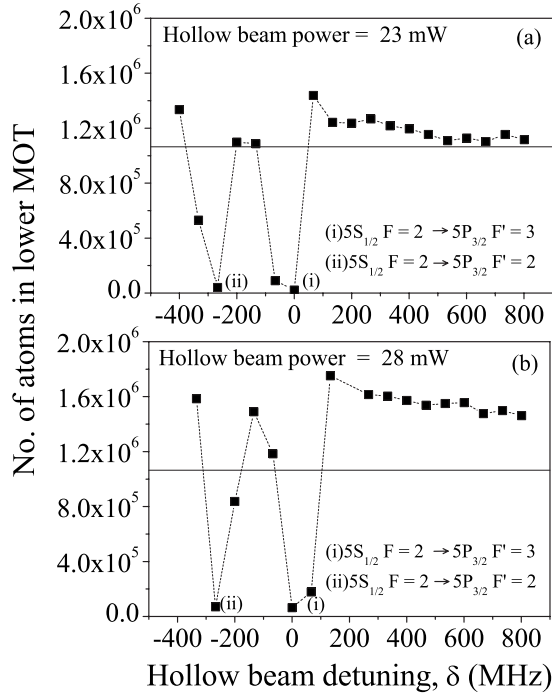


FIG. 3. Measured variation of number of atoms in the lower MOT with detuning of the hollow beam frequency (a) at a hollow beam power of 23 mW and (b) at a hollow beam power of 28 mW. The squares show the measured values, and dashed curves are for guiding the eye to the measured data. The horizontal lines show the number in the absence of a hollow beam.

variation of the number of atoms in the upper MOT with detuning of the hollow beam (for a power ~ 28 mW) is shown in Fig. 4.

The experimental results thus showed enhancement in the number of trapped atoms in both MOTs in the presence of the hollow beam. In an earlier work on the Cs MOT [29], the increase in the number of trapped atoms in the MOT due to the presence of an auxiliary control beam aligned within the capture volume was reported. In this work, it was suggested

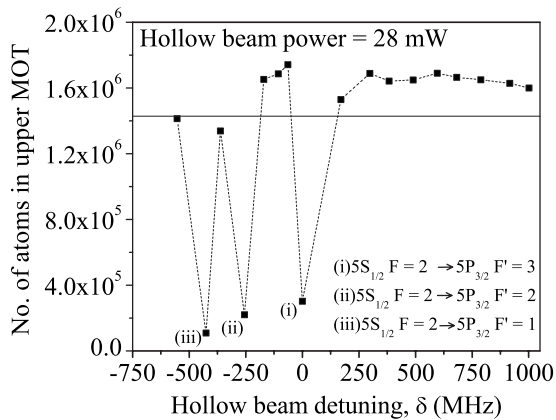


FIG. 4. Variation of the number of atoms in the upper MOT with detuning of the hollow beam frequency. The squares show the measured values and the dashed curve is to guide the eye to the measured data. The horizontal line shows the number in the absence of a hollow beam.

that the enhancement was due to optical pumping by the control beam among Zeeman sublevels, which removed the inaccessibility of atoms to the trapping beams occurring due to large Zeeman shifts at positions away from the MOT center. As the hollow beam diameter at the upper MOT was smaller (~ 3.2 mm) than the size of the trapping region (~ 10 mm), we believe that a similar optical pumping mechanism could be responsible for the increased number of atoms in the upper MOT. In contrast to the results in Ref. [29], we observed the destruction of the atom cloud with a very small number of atoms remaining there (see Fig. 4) when the hollow beam was resonant to the atomic transitions.

The observed enhancement in the number of trapped atoms in the lower MOT could be partly a result of more trapped atoms in the upper MOT, but cannot be fully explained by this. Comparison of Figs. 3 and 4 shows that while the maximum enhancement is $\sim 28\%$ for the upper MOT, that for the lower MOT is $\sim 71\%$. Also, a mechanism similar to that responsible for more atoms in the upper MOT is unlikely to be important for the lower MOT as the size of the hollow beam at the lower MOT (~ 14.3 mm diameter) was much larger than the trapping region diameter (~ 7 mm). We believe that the observed additional enhancement for the lower MOT could be a result of a slowing down of atoms ejected from the upper MOT by the counterpropagating hollow beam. A similar cooling mechanism was suggested to be responsible for the observed enhancement in a MOT loaded using a dark center slowing beam in a Zeeman slower setup by Miranda *et al.* [30]. We note that although the peak-to-peak intensity diameter (~ 3.2 mm) of the hollow beam at the upper MOT position was much larger than the upper MOT cloud size (~ 0.54 mm FWHM), there was a finite intensity in the central region because of diffraction effects as can be seen from the intensity profiles in Fig. 2. Destruction of the upper MOT by a hollow beam resonant to the atomic transition seems a result of this intensity profile. At the push beam intensity of $\sim 10^3$ mW/cm² used in the experiments, the estimated scattering rate is $\sim 1.85 \times 10^7$ Hz and the corresponding acceleration of atoms is $\sim 1.1 \times 10^5$ m/s². This acceleration is expected to act on atoms only up to a distance of 5 mm below the upper MOT center because beyond this distance repumping beams cease to exist, so the atoms would be lost to the $F=1$ hyperfine ground state and would not scatter either the push beam or the hollow beam. Neglecting the upper MOT trapping force, the action of above acceleration of the push beam up to ~ 5 mm distance is expected to raise the speed of an atom to ~ 33 m/s after ejection from the upper MOT. This speed is slightly higher than the estimated value of ~ 25 m/s for the capture velocity of the lower MOT [31]. Thus some atoms which have a speed greater than the capture velocity of the lower MOT will not be trapped. In the presence of the hollow beam, however, these atoms would acquire a lower speed as a result of a reduced net accelerating force after ejection and, hence, may be trapped in the lower MOT. We note that for very low power of the hollow beam (~ 0.6 mW), enhancement of the number of atoms in the lower MOT was observed only for some negative δ values which is consistent with the asymmetry of the Doppler cool-

ing process with respect to laser detuning. The asymmetry was not evident at higher hollow beam powers as is the case for the results shown in Fig. 3. We believe that at higher powers, additional effects such as a reduction in the divergence of the atom flux because of a finite transverse force associated with the converging hollow beam and guiding for positive detunings may come into play, enabling more atoms to reach the capture volume of the lower MOT.

To conclude, the results of experiments to investigate the effect of a hollow beam on the performance of a double-MOT setup with two vertically separated MOTs have been presented. Significant enhancement in the number of atoms in both MOTs was observed for appropriate alignment of the hollow beam and for both negative and positive hollow beam frequency detunings from the cooling transition. The observed increase was much larger for the lower MOT, suggesting an increase in the transfer efficiency. It is suggested that the increase was due to a decrease in the average speed as well as an increase in the number of atoms reaching the capture volume of the lower MOT. This is believed to be a

result of a slowing down of atoms after ejection from the upper MOT by the oppositely traveling hollow beam and a reduction in the divergence of the atomic flux because of transverse cooling and guiding effects. However, to understand these results better further work is required. For example, it may be useful to model the MOT potential in the presence of a hollow beam to understand the enhancement in the upper MOT. Similarly, reversing the propagation direction of the hollow beam or using the hollow beam in the same configuration, but with larger detuning and higher power than used here, may resolve the contribution of dipole guiding by a hollow beam during atom transfer to the observed enhancement in the lower MOT. These may be future experiments which will require some modifications in the present setup.

The authors would like to thank L. Sudarsanam, T. Balasubramaniam, and C. Mukharjee for support in fabricating the axicon mirror and S. Sendhil Raja for fabrication of the tapered tube.

-
- [1] H. J. Metcalf and P. van der Straten, *Laser Cooling and Trapping* (Springer-Verlag, New York, 1999).
- [2] *Bose-Einstein Condensation in Atomic Gases*, Proceedings of the International School of Physics "Enrico Fermi," Course CXL, Varenna, 1998, edited by M. Inguscio, S. Stringari, and C. E. Wieman (IOS Press, Amsterdam, 1999).
- [3] M. H. Anderson, J. R. Ensher, M. R. Matthews, C. E. Wieman, and E. A. Cornell, *Science* **269**, 198 (1995).
- [4] K. B. Davis, M.-O. Mewes, M. R. Andrews, N. J. van Druten, D. S. Durfee, D. M. Kurn, and W. Ketterle, *Phys. Rev. Lett.* **75**, 3969 (1995).
- [5] M.-O. Mewes, M. R. Andrews, D. M. Kurn, D. S. Durfee, C. G. Townsend, and W. Ketterle, *Phys. Rev. Lett.* **78**, 582 (1997).
- [6] M. R. Andrews, C. G. Townsend, H.-J. Miesner, D. S. Durfee, D. M. Kurn, and W. Ketterle, *Science* **275**, 637 (1997).
- [7] I. Bloch, T. W. Hänsch, and T. Esslinger, *Phys. Rev. Lett.* **82**, 3008 (1999).
- [8] A. Peters, K. Y. Chung, and S. Chu, *Metrologia* **38**, 25 (2001).
- [9] D. Schneble, M. Hasuo, T. Anker, T. Pfau, and J. Mlynek, *J. Opt. Soc. Am. B* **20**, 648 (2003).
- [10] N. Gemelke, E. Sarajlic, Y. Bidel, S. Hong, and S. Chu, *Phys. Rev. Lett.* **95**, 170404 (2005).
- [11] K. E. Strecker, G. B. Partridge, and R. G. Hulet, *Phys. Rev. Lett.* **91**, 080406 (2003).
- [12] C. S. Adams and E. Riis, *Prog. Quantum Electron.* **21**, 1 (1997).
- [13] J. Piilo, K.-A. Suominen, and K. Berg-Sorensen, *Phys. Rev. A* **65**, 033411 (2002).
- [14] F. S. Cataliotti, L. Fallani, F. Ferlaino, C. Fort, P. Maddaloni, and M. Inguscio, *J. Opt. B: Quantum Semiclassical Opt.* **5**, S17 (2003).
- [15] B. DeMarco and D. S. Jin, *Science* **285**, 1703 (1999).
- [16] G. B. Partridge, W. Li, and R. I. Kumar, Yean-an Liao, and R. G. Hulet, *Science* **311**, 503 (2006).
- [17] M. W. Zwierlein, J. R. Abo-Shaeer, A. Schirotzek, C. H. Schunck, and W. Ketterle, *Nature (London)* **435**, 1047 (2005).
- [18] C. J. Myatt, N. R. Newbury, R. W. Ghrist, S. Loutzenhiser, and C. E. Wieman, *Opt. Lett.* **21**, 290 (1996).
- [19] K. Gibble, S. Chang, and R. Legere, *Phys. Rev. Lett.* **75**, 2666 (1995).
- [20] H. J. Lewandowski, D. M. Harber, D. L. Whitaker, and E. A. Cornell, *J. Low Temp. Phys.* **132**, 309 (2003).
- [21] J. Goldwin, S. Inouye, M. L. Olsen, B. Newman, B. D. DePaola, and D. S. Jin, *Phys. Rev. A* **70**, 021601(R) (2004).
- [22] C. Y. Park, M. S. Jun, and D. Cho, *J. Opt. Soc. Am. B* **16**, 994 (1999).
- [23] T. B. Swanson, D. Asgeirsson, J. A. Behr, A. Gorelov, and D. Melconian, *J. Opt. Soc. Am. B* **15**, 2641 (1998).
- [24] L. Cacciapuoti, A. Castrillo, M. de Angelis, and G. Tino, *Eur. Phys. J. D* **15**, 245 (2001).
- [25] E. Dimova, O. Morizot, G. Stern, C. G. Alzar, A. Fioretti, V. Lorent, D. Comparat, H. Perrin, and P. Pillet, *Eur. Phys. J. D* **42**, 299 (2007).
- [26] S. R. Mishra, S. K. Tiwari, S. P. Ram, and S. C. Mehendale, *Opt. Eng.* **46**, 084002 (2007).
- [27] C. G. Townsend, N. H. Edwards, C. J. Cooper, K. P. Zetie, C. J. Foot, A. M. Steane, P. Szriftgiser, H. Perrin, and J. Dalibard, *Phys. Rev. A* **52**, 1423 (1995).
- [28] D. A. Steck, rubidium 87 D line data, available online at <http://steck.us/alkalidata>
- [29] S. Pradhan, S. J. Gaur, K. G. Manohar, and B. N. Jagatap, *Phys. Rev. A* **72**, 053407 (2005).
- [30] S. G. Miranda, S. R. Muniz, G. D. Telles, L. G. Marcassa, K. Helmersson, and V. S. Bagnato, *Phys. Rev. A* **59**, 882 (1999).
- [31] V. S. Bagnato, L. G. Marcassa, S. G. Miranda, S. R. Muniz, and A. L. de Oliveira, *Phys. Rev. A* **62**, 013404 (2000).